High dielectric constant and tunability of strontium titanate ceramics modified by chromium doping

2008 J. Phys.: Condens. Matter 20 415224

(http://iopscience.iop.org/0953-8984/20/41/415224)

J. Phys.: Condens. Matter **20** (2008) 415224 (8pp) doi:10.1088/0953-8984/20/41/415224

High dielectric constant and tunability of strontium titanate ceramics modified by chromium doping

Alexander Tkach, Olena Okhay, Paula M Vilarinho[1] and Andrei L Kholkin

Department of Ceramics and Glass Engineering, CICECO, University of Aveiro, 3810-193 Aveiro, Portugal

E-mail: paula.vilarinho@ua.pt

Received 4 May 2008, in final form 26 August 2008
Published 22 September 2008
Online at stacks.iop.org/JPhysCM/20/415224

Abstract

The incorporation of chromium on the strontium site of the perovskite lattice of $SrTiO_3$ ceramics and its influence on the structural, microstructural and low-frequency dielectric properties is studied in this work. Dense $Sr_{1-1.5x}Cr_xTiO_3$ ($x = 0, 0.0005, 0.0010, 0.0015$) ceramics are prepared from powders obtained by a sol–gel method. The lattice parameter $\sim$3.906 Å and average grain size $\sim$2.5 μm are almost identical for all the ceramic samples under study. On the other hand, the dielectric constant increases from approximately 7000 for $x = 0$ to >16 000 for $x = 0.0005$. Detailed investigations of the low-temperature dielectric properties show a remarkable increase of the tunability and nonlinearity of the dielectric constant as a function of dc bias field in strontium titanate ceramics modified by chromium doping but no ferroelectric or relaxor-like behaviour. These results imply the possible incorporation of small Cr amounts on the Sr site of strontium titanate ceramics and expand the tunable applications of $SrTiO_3$-based materials.

1. Introduction

For tunable capacitors and microwave device components, such as filters and phase shifting elements for phased array antennas, a dielectric material with high permittivity, excellent tunability and small loss (high Q) is desired [1, 2]. To transfer a large quantity of digital data within a bandwidth, frequency-hopping techniques based on high dielectric tunable materials will be needed in communication devices. On the other hand, the dielectric loss of the material has a significant impact on the speed and quality of the transmitted waves through the microwave component. High-Q dielectrics permit the fabrication of low power consumption components with enhanced battery life and minimized dimensions. However, achieving high tunability of the dielectric constant and low dielectric loss in one material is particularly challenging. Currently, the materials considered for practical tunable microwave applications belong to the $Ba_{1-x}Sr_xTiO_3$ solid solution system for applications at room temperature [3] and to $SrTiO_3$ (ST) for uses at cryogenic temperatures [4]. In spite of the requirement for operating at low temperatures that may limit the practical applications, $SrTiO_3$ is particularly attractive because of its high quality factor, Q. In contrast, $Ba_{1-x}Sr_xTiO_3$ solid solutions exhibit high microwave loss and also high thermal instability, which are enhanced with increasing $BaTiO_3$ concentration [1, 2]. Within the high dielectric permittivity materials, it is well known that a high thermal stability can be obtained in ferroelectrics with diffuse phase transitions or relaxors. The relaxor behaviour has been mainly observed in perovskite lead-based compositions such as $Pb(Mg_{1/3}Nb_{2/3})O_3$, $Pb(Sc_{1/2}Nb_{1/2})O_3$ and $Pb_{1-x}La_x(Zr_{1-y}Ti_y)O_3$, among others, in which more than one type of ions occupy the equivalent six-coordinated crystallographic sites [5]. However, high dielectric permittivity lead-free compositions are currently of great interest due to the need for environmental harmless applications.

The perovskite strontium titanate ($SrTiO_3$, ST) is an incipient ferroelectric material [6], i.e. it possesses polar soft modes but does not exhibit any ferroelectric phase

[1] Author to whom any correspondence should be addressed.

transition down to 0 K. It is known that the dielectric response and other related properties of $SrTiO_3$ can be modified by controlling the Sr/Ti ratio [7] and oxygen vacancy concentration [8], by oxygen isotope exchange [9] and by doping and substituting Sr and/or Ti ions [10–19]. In general Ti-site dopants, such as isovalent Zr^{4+}, Sn^{4+}, Ge^{4+} and Mn^{4+}, as well as heterovalent Mg^{2+} yield only a decrease of the low-temperature dielectric permittivity [10–12]. In contrast, isovalent Sr-site dopants, such as Ca^{2+}, Ba^{2+}, Pb^{2+}, Cd^{2+} and Mn^{2+} as well as heterovalent Bi^{3+} induce a dielectric anomaly [13–19], increasing the dielectric tunability at relatively high temperatures. Meanwhile, no systematic studies have been devoted to ST doped with Cr^{3+} on Sr sites and its dielectric properties. Probably the absence of this analysis is related to the fact that the occupation of Sr sites by Cr ions might be strongly restricted due to the considerable difference between the ionic radii of Cr^{3+} and Sr^{2+} [20]. The only known work covering ST doped with Cr on Sr sites is a recent report by Wang *et al* [21], stating the enhanced absorption of visible light for polycrystalline $Sr_{0.95}Cr_{0.05}TiO_3$ powders, where the substitution of small Cr cations for large Sr^{2+} is confirmed by the slightly shifted position of the (110) x-ray diffraction peak towards a higher 2θ value, compared to undoped $SrTiO_3$ and $SrTi_{0.95}Cr_{0.05}O_3$. However, a secondary phase, which can be detected in the x-ray diffraction patterns of [21], implies a low solid solubility limit of Cr cations on Sr sites of ST lattice. Indeed, the solid solubility limit is known to be as low as the size difference between the host and dopant ions is. In $Sr_{1-1.5x}A^{3+}_xTiO_3$ systems, the solubility limit for La^{3+} and Y^{3+} ions with ionic sizes 0.15 Å and 0.28 Å smaller than Sr^{2+} [20] is about $x = 0.20$ [22] and $x = 0.04$ [23], respectively. Accordingly, for Cr^{3+} ions with an ionic size 0.56 Å smaller than Sr^{2+} [20], the solubility limit is expected to be much less. Moreover, the radius of Cr cations (usually stable as a trivalent ion (Cr^{3+}) in the $3d^3$ high-spin configuration ($S = 3/2$)) in octahedral coordination is close to that of Ti^{4+} [20] and there are several publications in which a Cr^{3+} dopant was reported to occupy Ti sites in $SrTiO_3$. These works describe the modification of the conductivity [24], magnetoresistance [25] and ferromagnetism [26], the induction of photoluminescence [27] and the introduction of spin markers for electron spin resonance characterization [28] in ST-based materials. Currently, Cr-doped ST is attracting scientific and technical interest because it exhibits also an insulator-to-conductor behaviour transition with a resistive memory effect, with possible applications for nonvolatile random-access memories [29].

In this work $Sr_{1-1.5x}Cr_xTiO_3$ ceramics with small dopant concentrations $x = 0$, 0.0005, 0.0010 and 0.0015 are fabricated using fine-sized powders prepared by sol–gel. The influence of Cr content on the structural, microstructural, dielectric and ferroelectric properties of the $Sr_{1-1.5x}Cr_xTiO_3$ ceramics is systematically examined and discussed. The electric-field dependence of the dielectric permittivity of the ceramics is explored for possible application as tunable components.

2. Experimental procedure

$Sr_{1-1.5x}Cr_xTiO_3$ ($x = 0$, 0.0005, 0.0010, 0.0015) powders were obtained from stable stock solutions prepared by a sol–gel method. Advantages of the use of this chemical synthesis method are related to its relative simplicity, easy control of the composition stoichiometry, low level of impurities and low cost. $Sr_{1-1.5x}Cr_xTiO_3$ ($x = 0$, 0.0005, 0.0010, 0.0015) solutions with a concentration of about 0.2 M l^{-1} were prepared using strontium acetate (98%, ABCR, Germany), tetra-n-butyl orthotitanate (98%, Merck, Germany) and chromium acetate (99.5%, Merck, Germany) as starting precursors. Acetic acid (99.8%, Merck, Germany), 1,2-propanediol (99.5%, Riedel-de Haën, Germany) and absolute ethanol (99.8%, Merck, Germany) were used as solvents. Strontium acetate was initially dissolved in heated acetic acid (60 °C) followed by the addition of chromium acetate under constant stirring to form a transparent solution. After cooling to room temperature the former solution was diluted in 1,2-propanediol and titanium isopropoxide was added. The resultant clear solution was continuously stirred during 12 h in a closed flask and ethanol was added as a final step. $Sr_{1-1.5x}Cr_xTiO_3$ powders were then obtained by drying the solution in an oven at 80 °C for 36 h followed by calcination of the obtained gels at 950 °C for 20 h. The calcined powders were milled in a planetary mill using teflon pots, zirconia balls and alcohol. The particle size distribution of milled powders was determined by a Coulter LS 230 apparatus. Long-time milling (7 h) yields particle sizes between 0.04 and 0.6 μm and a considerable decrease of the content of agglomerates, whose particle sizes vary between 1 and 10 μm as seen from figure 1(a) for undoped $SrTiO_3$. Although agglomerates were not eliminated completely, the milling time was not further increased due to the rising risk of contamination (namely with zirconia from the milling media). Pellets of ~10 mm in diameter were uniaxially pressed at 100 MPa and isostatically pressed at 200 MPa. Sintering studies indicated that the ceramics density increases with the sintering temperature, as shown in figure 1(b). The sintering was carried out at 1550 °C in air with heating and cooling rates of 5 °C min^{-1} and a dwelling time of 5 h. Selected samples for dielectric characterization were sintered in oxygen and nitrogen flows as well. In comparison with the ceramics prepared by a conventional mixed oxide method [7], this 'moderate' density of 95% obtained at such an elevated sintering temperature is probably related to the degree of agglomeration of the submicron-sized particles obtained by sol–gel. The relative density of $Sr_{1-1.5x}Cr_xTiO_3$ ceramics is indicated in table 1, showing that the introduction of Cr ions on Sr sites slightly promotes the densification up to 96% for $x = 0.0005$, followed by a decrease to 92% for $x = 0.0015$. Densities of the sintered samples were measured by Archimedes' method using diethylphthalate as the immersion liquid.

A x-ray diffractometer (Rigaku D/Max-B) with Cu Kα source ($\lambda = 1.540\,562$ Å), operated at 40 kV and 30 mA, was used for the identification of crystal phases on grounded sintered samples. A step size of 0.02°, a scan rate of 1° min^{-1} and scan ranges of 20°–108° were used. Lattice parameters

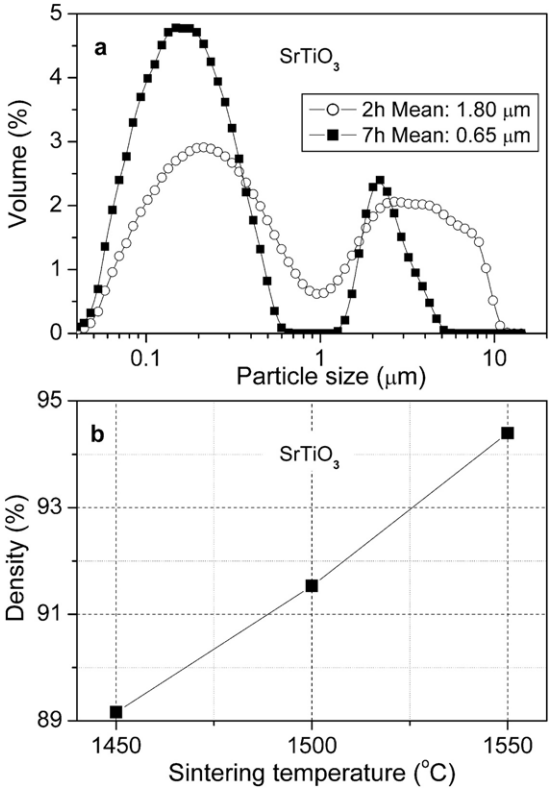

Figure 1. Particle size distribution of $SrTiO_3$ powders after 2 h (open circles) and 7 h (solid squares) of milling (a). Density of $SrTiO_3$ ceramics as a function of sintering temperature (b).

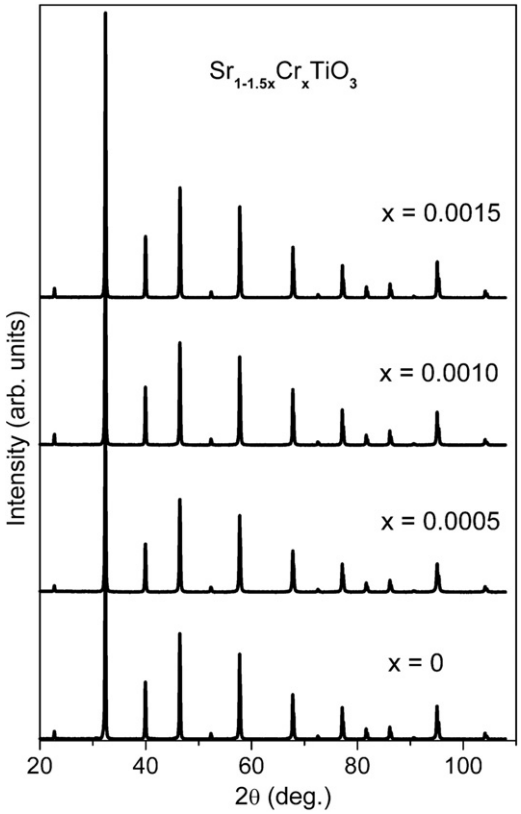

Figure 2. XRD patterns of sintered $SrTiO_3$, $Sr_{0.99925}Cr_{0.0005}TiO_3$, $Sr_{0.99850}Cr_{0.0010}TiO_3$ and $Sr_{0.99775}Cr_{0.0015}TiO_3$ ceramics.

Table 1. Relative density, lattice parameter and average grain size of $SrTiO_3$, $Sr_{0.99925}Cr_{0.0005}TiO_3$, $Sr_{0.99850}Cr_{0.0010}TiO_3$ and $Sr_{0.99775}Cr_{0.0015}TiO_3$ ceramics sintered at 1550 °C for 5 h.

Composition	Density (%)	Lattice parameter (Å)	Average grain size (μm)
$SrTiO_3$	∼94.5	3.906 31(8)	∼2.4
$Sr_{0.99925}Cr_{0.0005}TiO_3$	∼96	3.905 80(8)	∼2.2
$Sr_{0.99850}Cr_{0.0010}TiO_3$	∼94	3.905 88(7)	∼2.7
$Sr_{0.99775}Cr_{0.0015}TiO_3$	∼92	3.905 99(6)	∼2.4

were calculated by a least-squares-approach fitting of the x-ray diffraction (XRD) data using Rietveld refinement WinPLOTR software.

A scanning electron microscope (SEM, Hitachi S-4100), operating at 20 kV, and a transmission electron microscope (TEM, Hitachi 9000), operating at 300 kV, and both equipped with energy-dispersive spectroscopes (EDS) were used to observe the microstructure and determine qualitative chemical compositional analysis of the ceramics. SEM/EDS analysis was performed on polished and thermally etched sections of sintered samples, whereas TEM/EDS analysis was carried out on the samples ground to approximately 30 μm thick and ion-beam-milled using a BAL-TEC Ion Mill (RES 100). Average grain size of the sintered pellets was measured on SEM micrographs by AnalySIS (Soft Imaging System GmbH) software.

For the dielectric measurements, sintered samples were polished to a thickness of ∼0.45 mm and gold electrodes were sputtered on both sides. The dielectric permittivity and loss were measured at different frequencies between 100 Hz and 1 MHz, using a precision LCR-meter (HP 4284A). Measurements in the temperature range of 10–300 K were performed during heating up at a rate of 0.75 K min^{-1} in an He closed cycle cryogenic system (Displex ADP-Cryostat HC-2). Hysteresis $P(E)$ loops were measured at low temperatures under applied ac fields sinusoidally varying between about −15 and 15 kV cm^{-1} with a frequency of 50 Hz, using a standard Sawyer–Tower circuit and a digital oscilloscope (LeCroy LT322). DC electric-field dependences of the dielectric permittivity were measured at fixed temperatures, at which the sample was allowed to reach thermal equilibrium for at least 30 min. The measurements of the dielectric permittivity under bias ranging from 0 to ∼20 kV cm^{-1} were performed at 10 kHz using the precision LCR-meter (HP 4284A), a blocking circuit and a high-voltage power supply (Glassman PS/EH10P10.0-22).

3. Results and discussion

Figure 2 shows the XRD patterns of the sintered ceramic samples. For all the compositions the observed x-ray diffraction lines are consistent with the cubic crystallographic structure of undoped ST and no second phases were observed. The lattice parameters calculated by Rietveld refinement of the XRD data are indicated in table 1. For both undoped and Cr-doped ST, the lattice parameter was found to be

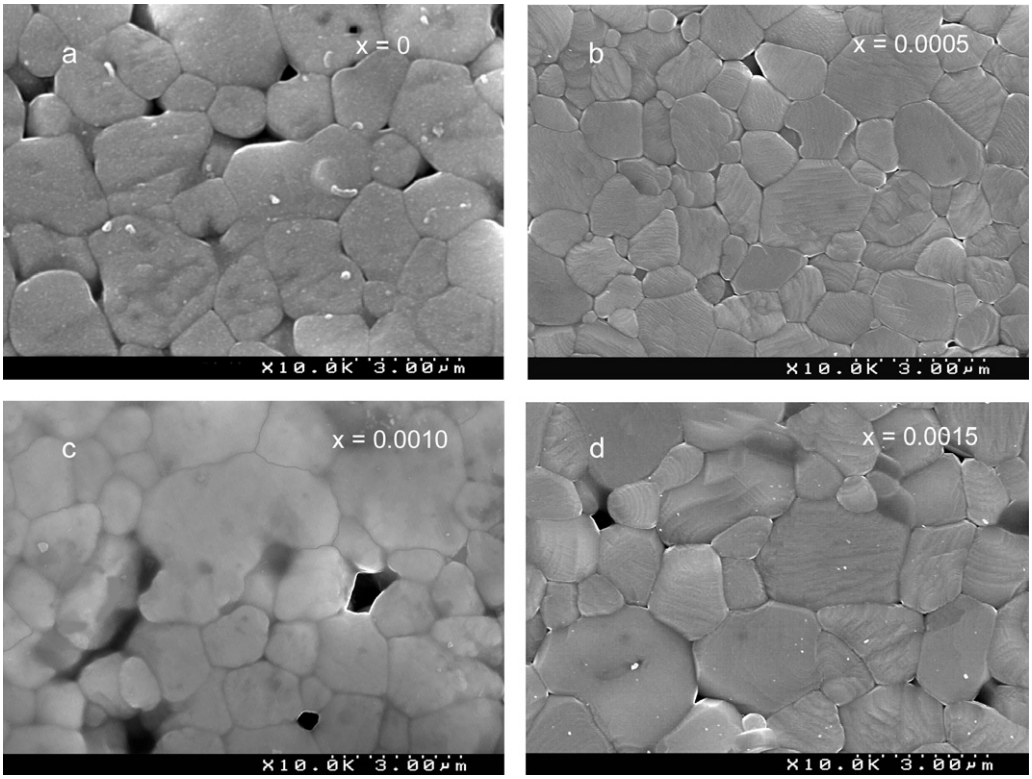

Figure 3. SEM micrographs of $SrTiO_3$ (a), $Sr_{0.99925}Cr_{0.0005}TiO_3$ (b), $Sr_{0.9985}Cr_{0.0010}TiO_3$ (c) and $Sr_{0.99775}Cr_{0.0015}TiO_3$ (d) ceramics.

~3.906 Å, which is in close agreement with the literature data for $SrTiO_3$ [19]. From ionic size consideration [20], a lattice contraction should occur for the substitution of Sr^{2+} by smaller Cr^{3+} ions, similar to the reported lattice variation of $Sr_{1-x}Ca_xTiO_3$ with increasing x [19]. However, due to the significant difference between the size of Sr^{2+} and Cr^{3+}, the solid solubility limit is expected to be quite small. Indeed, the limited solid solubility might explain the observed absence of a marked decrease of the lattice parameter in the $Sr_{1-1.5x}Cr_xTiO_3$ system, in spite of the fact that no second phases could be detected either by XRD or even by TEM/EDS analysis. Only slim and clean grain boundaries were observed by TEM. Similar lattice parameter invariance with the doping content was reported for $Sr_{1-x}Mg_xTiO_3$ ceramics and attributed to a very low solubility limit of Mg in the $SrTiO_3$ lattice due to the instability of the small Mg^{2+} cations with twelvefold coordination in the cubic perovskite lattice [12].

Figure 3 depicts a sequence of SEM microstructures of $Sr_{1-1.5x}Cr_xTiO_3$ as a function of Cr content. The images reveal relatively dense ceramics in accordance with the density measurements. The grain size of the ceramics varies from 0.2 to 8 μm with a normal distribution. The average grain size of Cr-doped ST ceramics (2.5 μm) is close to that of undoped ST (2.4 μm), as also presented in table 1.

The results of the low-frequency dielectric measurements are summarized in figures 4(a)–(c). The temperature (T) dependence of the dielectric constant ε' for $SrTiO_3$, $Sr_{0.99925}Cr_{0.0005}TiO_3$, $Sr_{0.99850}Cr_{0.0010}TiO_3$ and $Sr_{0.99775}Cr_{0.0015}TiO_3$ is shown in figure 4(a) at 10 kHz. No dispersion of the dielectric constant was detected in the frequency range 10^2–10^6 Hz. A steep increase of the ε' and a levelling-off at high values, as the temperature approaches 0 K with no obvious dielectric permittivity anomaly, was observed for undoped ST, as a typical quantum paraelectric [6]. Dielectric behaviour of Cr-doped ST samples is qualitatively similar to that of undoped ST and reveals no anomalies. However, there is a remarkable increase of the low-temperature dielectric constant from approx. 7000 up to 16 000 (for the Cr concentration $x = 0.0005$). The observed increase of the dielectric permittivity can be due to intrinsic effects, related to the incorporation of Cr on the ST host lattice or due to extrinsic effects that include the development of Schottky barriers between semiconductive grains at insulating grain boundaries (interfacial/grain boundary effect), composition stoichiometry variations and density of the ceramics. The interfacial/grain boundary effect is characterized by a dielectric relaxation associated with electric dipoles created when, under an applied electric field, conducting carriers in the semiconductive grain interior are blocked by the insulating boundary layer. Such relaxation strongly increases the dielectric permittivity in the high-temperature range (above 50 K) [30]. However, in the present study, no dielectric relaxation is observed and the dielectric permittivity increases mainly in the low-temperature range (below 50 K). An increase of the dielectric permittivity at low temperatures was also observed in ST ceramics with slight Ti excess [7]. The presence of such Ti excess is possible for Cr-doped ST, if one supposes that Cr was not incorporated in the ST lattice or if it occupies Ti sites. However, the increase of the dielectric constant observed in the present study in the

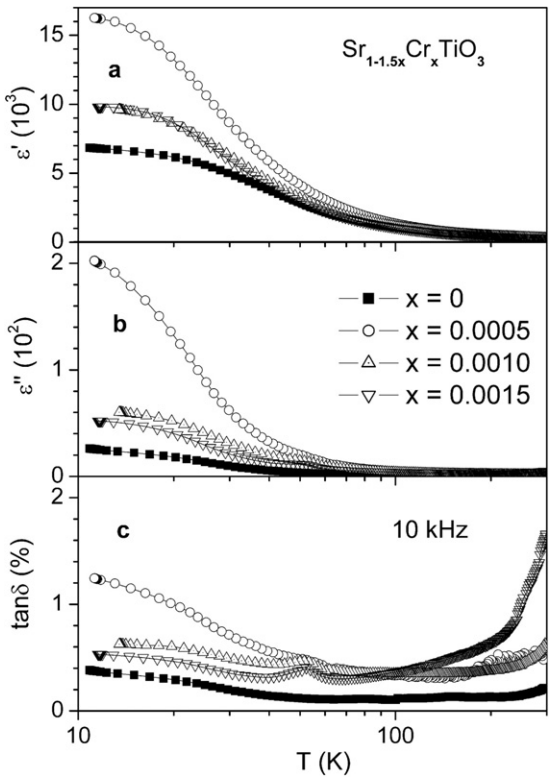

Figure 4. Temperature dependence of real ε' (a) and imaginary ε'' (b) parts of dielectric permittivity and of tan δ (c) at 10 kHz for $SrTiO_3$, $Sr_{0.99925}Cr_{0.0005}TiO_3$, $Sr_{0.99850}Cr_{0.0010}TiO_3$ and $Sr_{0.99775}Cr_{0.0015}TiO_3$ ceramics.

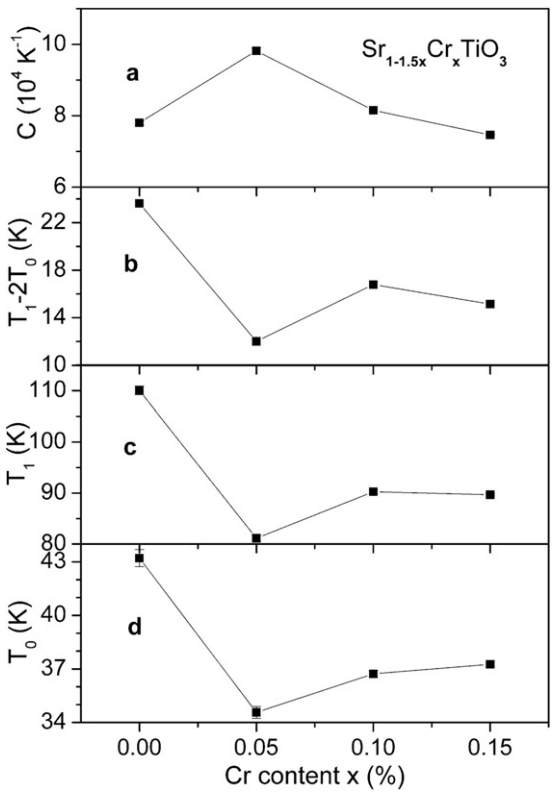

Figure 5. Barrett law parameters: Curie–Weiss constant C (a), ferroelectric state signature $T_1 - 2T_0$ (b), temperature of the crossover between classical and quantum behaviour T_1 (c) and the transition temperature at which the lattice instability would occur in the absence of quantum fluctuations T_0 (d) for $Sr_{1-.5x}Cr_xTiO_3$ ceramics as a function of Cr content.

low-T region is one order of magnitude higher than the one reported for Ti-excess ST ceramics. So it seems unlikely that the observed increase of the dielectric permittivity is solely a non-stoichiometry effect. Moreover, Ti-site dopants are known to decrease the low-temperature dielectric permittivity [10–12]. Another reason for the observed augment in the dielectric constant of $Sr_{0.99925}Cr_{0.0005}TiO_3$, can be related to the relatively higher density of these samples (96%) when compared with undoped ST ceramics (94.5%). However, as also seen in figure 4, though further increases of Cr content x to 0.0010 and 0.0015 result in the decrease of the ceramics density (from 94% for $Sr_{0.99850}Cr_{0.0010}TiO_3$ to 92% for $Sr_{0.99775}Cr_{0.0015}TiO_3$), it results in the stabilization of the maximum value of the dielectric constant around 10 000; a value that is still higher than that of undoped ST. So, it looks like that there is no direct correlation between sample density and their maximum of the dielectric permittivity, and further measurements and analyses of the dielectric response were then performed.

Dielectric constant data were fitted to the Barrett law:

$$\varepsilon' = C/[(T_1/2)\coth(T_1/2T) - T_0] \qquad (1)$$

where C stands for the Curie–Weiss constant, T_1 stands for the temperature of the crossover between classical and quantum paraelectric behaviour and T_0 stands for the transition temperature at which the lattice instability would occur in the absence of quantum fluctuations [31]. Barrett law parameters are plotted in figure 5 as a function of Cr content. The Curie–Weiss constant C, shown in figure 5(a), is higher for Cr-doped ST than that for undoped ST ceramics and reveals a maximum for $x = 0.0005$, reflecting the highest dielectric constant observed in the $Sr_{1-1.5x}Cr_xTiO_3$ system. On the other hand, the $(T_1 - 2T_0)$ parameter, indicative of the ferroelectric state of the system (figure 5(b)) and obtained using fitted values of T_1 (figure 5(c)) and T_0 (figure 5(d)), decreases with Cr doping and shows a minimum for the Cr content of 0.05%. The diminishing of $(T_1 - 2T_0)$ towards zero indicates an approximation to the ferroelectric behaviour, i.e. polar ordering becomes stronger with respect to quantum fluctuations [6, 32]. Thus, the approximation to a polar state for ST samples doped with small content of Cr, namely for $x = 0.0005$, is clearly seen. A similar effect was reported for $Sr_{1-x}Ca_xTiO_3$ single crystals, where $(T_1 - 2T_0)$ was shown to reach -1 K for $x = 0.007$ [32] and the dielectric constant at 10 K was found to increase from ∼24 000 for $x = 0$ to ∼57 000 for $x = 0.002$ [13]. Further increase of the Ca concentration up to $x < 0.015$ led to the formation of sharp peaks in the temperature dependence of the dielectric permittivity and the phenomenon was attributed to polar off-centre displacement of small calcium ions in large strontium sites [13, 32]. An equivalent mechanism may also be applied to Cr-doped ST, in which Cr^{3+} ions are much smaller than the Sr^{2+} host. However, in contrast to Ca-doped ST, the enhanced dielectric response of Cr-doped ST ceramics does not transform into a dielectric anomaly, probably due to the limited solid solubility of Cr^{3+}

on Sr sites of ST. The observed decrease of the dielectric constant upon further increase in Cr content is consistent with the assumption of the low solubility limit and a possible segregation of Cr.

The temperature dependence of the dielectric loss, $\tan\delta$, shown in figure 4(c), reveals values lower than 0.004 for undoped ST and lower than 0.017 for Cr-doped ST. Rather low loss values for undoped ST ceramics can be a reflection of the high purity levels of the sol–gel-derived powders used for ceramics fabrication. Increase of dielectric loss for Cr-doped ST samples at low temperatures can be explained by the approximation to a ferroelectric state for low dopant concentration, whereas high loss at room temperature (increasing with Cr content) might come from the increasing conductivity due to charge carriers associated with Cr doping [24]. No peaks were observed in the temperature dependence of loss for undoped ST, while a clear frequency-dependent peak is present for Cr-doped samples. At 10 kHz this peak is located around 55 K for all the chromium concentrations. A number of works reported a similar peak for undoped ST and related it to an elastic multi-domain state, appearing below the octahedral tilt phase transition at ~108 K [33, 34]. No peak in this temperature range was observed for single-domain ST crystals by cooling under an electric field [35]. In the present study the grains of undoped ST ceramics seem small enough to be in a single-domain state. However, although Cr doping does not have a considerable effect on the grain size, it is accompanied by the formation of strontium vacancies. Meanwhile Sr vacancies are known as domain pinning defects and as a source of the lattice distortions, favouring the tilt of the oxygen octahedra [36]. Thus, the presence of Sr vacancies, besides strengthening the octahedral tilt phase transition, favours the elastic multi-domain state, which might explain the loss peak observed in this work around 55 K at 10 kHz.

The effect of the sintering atmosphere on the dielectric properties of Cr-doped ST ceramics was also analysed. No significant differences were found between the dielectric responses of the samples sintered in air, oxygen and nitrogen. The only dissimilarity was the vanishing of the peak around 55 K in the temperature dependence of dielectric loss for ceramics sintered in nitrogen atmosphere. Such behaviour seems to be related to the suppression of the octahedral tilt transition and elimination of the elastic domains due to the formation of oxygen vacancies and clearly support the preceding discussion. Oxygen octahedra rotations are cooperative and induce a phase transition by a cogwheel motion from one octahedron to the next via the shared O-ion corner. Therefore, the presence of O vacancies statistically reduces the possibility of coupling of rotations of octahedra, suppressing the transition and preventing the elastic multi-domain state [36].

In order to complete the electric characterization, the polarization P as a function of electric field E was evaluated. Figure 6 displays the P versus E hysteresis curves for $Sr_{0.99925}Cr_{0.0005}TiO_3$ and $SrTiO_3$ ceramics at 16 (figure 6(a)) and 28 K (figure 6(b)). Both samples reveal, at these low temperatures, very slim S-shaped loops with remnant

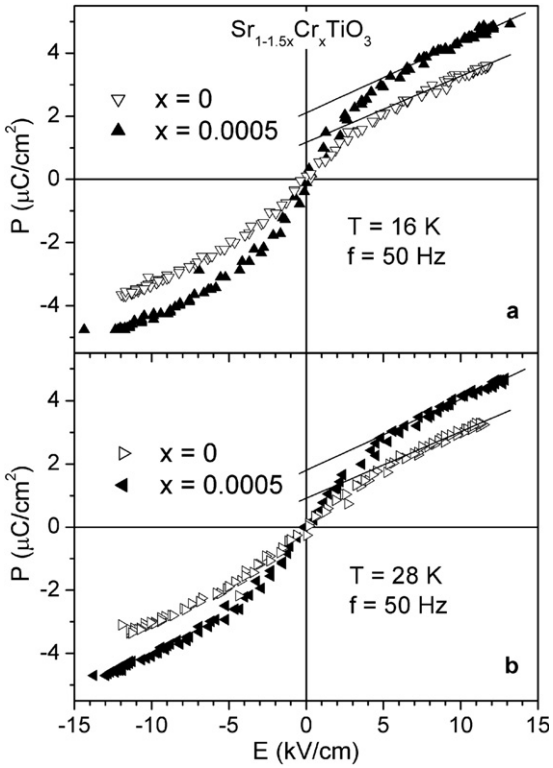

Figure 6. P versus E hysteresis curves of $SrTiO_3$ (open symbols) and $Sr_{0.99925}Cr_{0.0005}TiO_3$ (solid symbols) ceramics at 16 K (a) and 28 K (b) and 50 Hz.

polarization P_r close to zero. Nonlinearity of P versus E curves increases with decreasing temperature, suggesting the approximation to a polar state. At constant temperature, however, the nonlinearity for $Sr_{0.99925}Cr_{0.0005}TiO_3$ is higher than that of undoped $SrTiO_3$ ceramics. Quantitatively it can be displayed by the increase of the saturation polarization P_s value, obtained by the linear extrapolation of data above 5 kV cm^{-1} to zero field, as shown by the straight lines in figure 6. For $Sr_{0.99925}Cr_{0.0005}TiO_3$ ceramics, P_s is 2.1 μC cm^{-2} at 16 K and 1.8 μC cm^{-2} at 28 K. In comparison, for $SrTiO_3$ ceramics, P_s is 1.2 μC cm^{-2} at 16 K and 0.9 μC cm^{-2} at 28 K, i.e. twice as small. This behaviour apparently results in the strengthening of polar ordering with respect to quantum fluctuations by Cr doping, in accordance with the fitting of the dielectric constant to the Barrett law.

Figure 7 shows the bias-field dependence of the relative tunability n_r of $Sr_{1-1.5x}Cr_xTiO_3$ ceramics with $x = 0$ and 0.0005, defined as $n_r = [\varepsilon'(0) - \varepsilon'(E_b)]/\varepsilon'(0)$, where $\varepsilon'(0)$ stands for the dielectric constant at zero field and $\varepsilon'(E_b)$ stands for the dielectric permittivity under applied bias field E_b. The dielectric constant of both samples is tunable at low temperatures and upon the temperature increase to room temperature, tunability decreases almost down to zero. The enhancement of n_r with the introduction of Cr into the Sr site of $SrTiO_3$ is drastic, especially in the bias-field range of $E_b < 10$ kV cm^{-1}. The tunability of $Sr_{0.99925}Cr_{0.0005}TiO_3$ at 15 K could reach ~89% under a bias field of 20 kV cm^{-1} (figure 7(b)). It is ~77% under 7 kV cm^{-1}. Comparatively, the relative tunability n_r of $SrTiO_3$ at the same temperature (15 K)

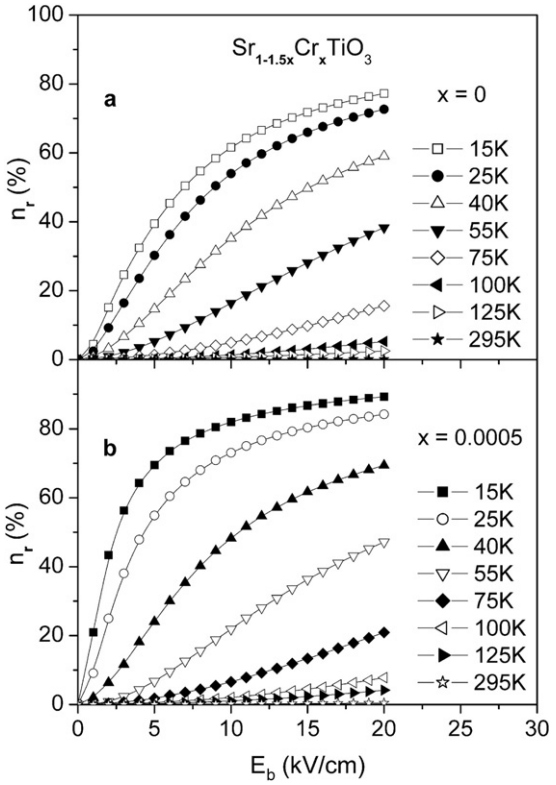

Figure 7. Field dependence of relative tunability $n_r = [\varepsilon'(0) - \varepsilon'(E_b)]/\varepsilon'(0)$ of $SrTiO_3$ (a) and $Sr_{0.99925}Cr_{0.0005}TiO_3$ (b) ceramics at 10, 25, 40, 55, 75, 100, 125 and 295 K and 10 kHz.

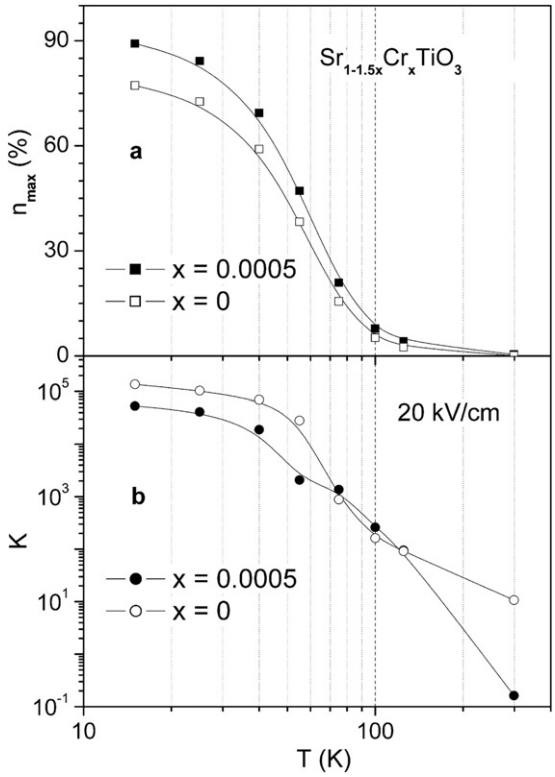

Figure 8. Relative tunability n_{max} (a) and communication quality factor K (b) of $SrTiO_3$ and $Sr_{0.99925}Cr_{0.0005}TiO_3$ ceramics under 20 kV cm^{-1} at 10 kHz as functions of temperature.

and bias field (7 kV cm^{-1}) is 1.5 times smaller (figure 7(a)) and reaches ∼77% just under a bias field of 20 kV cm^{-1}. Thus, a rather small incorporation of Cr into the Sr site of ST ceramics results in a significant enhancement of the tunability and a large reduction of the driving electric field even at elevated temperatures, comparing with undoped ST.

The relative tunability under the maximum electric field of 20 kV cm^{-1}, n_{max}, as a function of temperature is presented in figure 8(a) for $Sr_{1-1.5x}Cr_xTiO_3$ ceramics with $x = 0$ and 0.0005. Maximum relative tunability of the $Sr_{0.99925}Cr_{0.0005}TiO_3$ sample is higher than that of undoped ST in all of the temperature range, although the difference becomes smaller together with values of the tunability upon temperature increase.

Communication quality factor $K = (n-1)^2/[n \tan\delta(0) \tan\delta(E_{max})]$, where $n = \varepsilon'(0)/\varepsilon'(E_{max})$ stands for the tunability of the component [1], was also calculated to complete the analysis. The values of the loss factor measured at 10 kHz and under zero $[\tan\delta(0)]$ and maximum bias field of 20 kV cm^{-1} $[\tan\delta(E_{max})]$ were used in this equation. K of $SrTiO_3$ and $Sr_{0.99925}Cr_{0.0005}TiO_3$ ceramic samples is shown in figure 8(b) as a function of temperature. Very high values ∼10^5 were obtained at low temperatures. The communication quality factor for Cr-doped ST is somewhat lower than that of undoped ST due to the higher loss level.

Increase of loss, enhancement of tunability and reduction of driving electric field are indeed characteristic features of the approximation to a polar state.

4. Conclusions

Ceramic samples were synthesized by the sol–gel method according to $Sr_{1-1.5x}Cr_xTiO_3$ ($0 \leqslant x \leqslant 0.0015$) composition, in which intentional stoichiometric variations facilitate the incorporation of Cr ions into the Sr sites of the ST lattice.

From the structural and microstructural point of view no considerable differences were observed in the lattice parameter (∼3.906 Å), density (94 ± 2%) and grain size (2.45 ± 0.25 μm) for all the studied ceramics. However, from the dielectric response perspective a departure from the quantum paraelectric state and an approximation to a polar state were detected in $Sr_{1-1.5x}Cr_xTiO_3$ ceramics when x increased from 0 to 0.0005. Though a very small amount of Cr, it was enough to induce a remarkable increase of the low-temperature dielectric constant from approx. 7000 up to 16 000, as well as a significant enhancement of the nonlinearity of P and ε' versus E and a large reduction of driving electric field for the tunability of the dielectric permittivity. The approximation to a polar state is supposed to originate from the off-centre displacements of small chromium ions on large strontium sites of the highly polarizable ST lattice and to be controlled due to the very small solid solubility limit for the Cr^{3+} on the Sr sites. ST modified by small Cr incorporation into the Sr site is a promising material for possible tunable application as a phase shifter at cryogenic temperatures.

Acknowledgments

The authors acknowledge financial support from FEDER and the European Network of Excellence FAME under contract FP6-500159-1. OO acknowledges the FCT for financial support (SFRH/BD/19861/2004).

References

[1] Vendik O G, Hollmann E K, Kozyrev A B and Prudan A M 1999 *J. Supercond.* **12** 325
[2] Tagantsev A K, Sherman V O, Astafiev K F, Venkatesh J and Setter N 2003 *J. Electroceram.* **11** 5 and references therein
[3] De Flaviis F, Alexopoulos N G and Stafsudd O M 1997 *IEEE Trans. Microw. Theory* **45** 963
[4] Wooldridge I, Turner C W, Warburton P A and Romans E J 1999 *IEEE Trans. Appl. Supercond.* **9** 3220 and references therein
[5] Cross L E 1994 *Ferroelectrics* **151** 305
[6] Müller K A and Burkard H 1979 *Phys. Rev.* B **19** 3593
[7] Tkach A, Vilarinho P M, Senos A M R and Kholkin A L 2005 *J. Eur. Ceram. Soc.* **25** 2769
[8] Frederikse H P R, Thurber W R and Hosler W R 1964 *Phys. Rev.* **134** A442
[9] Itoh M, Wang R, Inaguma Y, Yamaguchi T, Shan Y J and Nakumura T 1999 *Phys. Rev. Lett.* **82** 3540
[10] Lemanov V V, Sotnikov A V, Smirnova E P and Weihnacht M 2002 *Phys. Solid State* **44** 2039
[11] Tkach A, Vilarinho P M and Kholkin A L 2004 *Ferroelectrics* **304** 917
[12] Tkach A, Vilarinho P M and Kholkin A 2004 *Appl. Phys.* A **79** 2013
[13] Bednorz J G and Müller K A 1984 *Phys. Rev. Lett.* **52** 2289
[14] Lemanov V V, Smirnova E P, Syrnikov P P and Tarakanov E A 1996 *Phys. Rev.* B **54** 3151
[15] Lemanov V V, Smirnova E P and Tarakanov E A 1997 *Phys. Solid State* **39** 628
[16] Guzhva M E, Lemanov V V and Markovin P A 2001 *Phys. Solid State* **43** 2146
[17] Tkach A, Vilarinho P M and Kholkin A L 2005 *Appl. Phys. Lett.* **86** 172902
[18] Ang C, Yu Z, Vilarinho P M and Baptista J L 1998 *Phys. Rev.* B **57** 7403
[19] Mitsui T and Westphal W B 1961 *Phys. Rev.* **124** 1354
[20] Shannon R D 1976 *Acta Crystallogr.* A **32** 751
[21] Wang D, Ye J, Kako T and Kimura T 2006 *J. Phys. Chem.* B **110** 15824
[22] Yu Z, Ang C and Cross L E 1999 *Appl. Phys. Lett.* **74** 3044
[23] Fu Q X, Mi S B, Wessel E and Tietz F 2008 *J. Eur. Ceram. Soc.* **28** 811
[24] Paek S H, Lee E S, Kim S H, Seong J Y, Mah J P, Park C S, Choi J S and Jung J H 1998 *J. Mater. Sci.* **33** 1239
[25] Inaba J and Katsufuji T 2005 *Phys. Rev.* B **72** 052408
[26] Zhang S X, Ogale S B, Kundaliya D C, Fu L F, Browning N D, Dhar S, Ramadan W, Higgins J S, Greene R L and Venkatesan T 2006 *Appl. Phys. Lett.* **89** 012501
[27] Trepakov V, Savinov M, Okhay O, Tkach A, Vilarinho P, Kholkin A, Gregora I and Jastrabik L 2007 *J. Eur. Ceram. Soc.* **27** 3705 and references therein
[28] Glinchuk M D, Bykov I P, Slipenyuk A M, Laguta V V and Jastrabik L 2001 *Phys. Solid State* **43** 841
[29] Karg S, Meijer G I, Widmer D and Bednorz J G 2006 *Appl. Phys. Lett.* **89** 072106 and references therein
[30] Lunkenheimer P, Fichtl R, Ebbinghaus S G and Loidl A 2004 *Phys. Rev.* B **70** 172102
[31] Barrett J H 1952 *Phys. Rev.* **86** 118
[32] Bianchi U, Dec J, Kleemann W and Bednorz J G 1995 *Phys. Rev.* B **51** 8737
[33] Viana R, Lunkenheimer P, Hemberger J, Bohmer R and Loidl A 1994 *Phys. Rev.* B **50** 601
[34] Mizaras R and Loidl A 1997 *Phys. Rev.* B **56** 10726
[35] Dec J, Kleemann W and Westwanski B 1999 *J. Phys.: Condens. Matter* **11** L379
[36] Tkach A, Vilarinho P M, Kholkin A L, Reaney I M, Pokorny J and Petzelt J 2007 *Chem. Mater.* **19** 6471 and references therein